

Fan-out in Gene Regulatory Networks

Kyung Hyuk Kim* and Herbert M. Sauro

Department of Bioengineering, University of Washington,
William H. Foege Building, Box 355061, Seattle, WA 98195-5061, U.S.A.

Abstract

In synthetic biology, gene regulatory circuits are often constructed by combining smaller circuit components. Connections between components are achieved by transcription factors acting on promoters. If the individual components behave as true modules and certain module interface conditions are satisfied, the function of the composite circuits can in principle be predicted. In this paper, we investigate one of the interface conditions: fan-out. We quantify the fan-out, a concept widely used in electric engineering, to indicate the maximum number of the downstream inputs that an upstream output transcription factor can regulate. We show that the fan-out is closely related to retroactivity studied by Del Vecchio, et al. We propose an efficient operational method for measuring the fan-out that can be applied to various types of module interfaces. We also show that the fan-out can be enhanced by self-inhibitory regulation on the output. We discuss the potential role of the inhibitory regulations found in gene regulatory networks and protein signal pathways. The proposed estimation method for fanout not only provides an experimentally efficient way for quantifying the level of modularity in gene regulatory circuits but also helps characterize and design module interfaces, enabling the modular construction of gene circuits.

* Corresponding Author: kkim@uw.edu

Running title: Fan-out in Gene Regulatory Networks

Character count: 53631

Background

Engineering relies on modular composition that is the ability to combine functional units with the knowledge that the intrinsic properties of each module is unaffected to a large degree by the composition. In biology we are less clear on the notion of a modular component, or at least biology has multiple definitions depending on context. Here we will define a module as a self-contained functional unit whose intrinsic properties are independent of the surrounding milieu. This definition is similar to that used in engineering. For example, the intrinsic properties of a TTL NAND gate [1] is unaffected (within certain design constraints) when connected to other TTL logic gates. That is, a NAND gate remains a NAND gate no matter what it is connected to. This property allows engineers to design, predict and fabricate complex circuits at very low cost. The question whether such self-contained and functionally independent modules exist at the biological cellular network level is still an ongoing research problem [2]. In this paper we will be concerned with the design of modular synthetic components [3–8] and avoid the question of modularity in natural complex systems.

In the most abstract sense we can define a module as follows. Given a functional unit M with input I and output O , we can define a relation between the input and output as $O = M(I)$. Given two functional units, M_1 and M_2 , where the output of M_1 serves as the input to M_2 , then M_1 and M_2 are defined as modules if the relation, $O_2 = M_2(M_1(I_1))$ is true. This simply means that in connecting M_1 and M_2 together, M_2 has no effect on the functional characteristics of M_1 and vice versa.

Predictable composition is of particular interest to the synthetic biology community where gene circuits are “wired” together via transcription factors (TFs) and corresponding promoters (Figure 1). This mode of wiring makes the physical construction of relatively complex networks possible [9, 10]. However the general question of whether making a connection between two genetic units results in a functional whole remains. In particular a number of issues present themselves that include independence from the surrounding milieu (also called orthogonality [4]): domain matching and impedance bridging. The former describes the situation where the operating concentration range of an output transcription factor matches the range of the input target. Impedance bridging, which is the main topic of this paper, is concerned with how much a downstream target circuit can affect the functional properties of an upstream unit. It is not to be confused with impedance matching which is related

to the maximum power transfer between two circuits. There has recently been interest in defining impedance bridging in genetic and protein circuits [11, 12] and a related quantity called retroactivity was introduced by Saez-Rodriguez et al. [13] and Del Vecchio et al. [14] to describe the effect of one module on another.

In electric engineering there exist guidelines and published constraints on how many electrical modules can be driven from a source. For example, one rule of thumb for analog circuits suggests that the impedance at the input should be ten times the impedance at the driving circuit. In digital circuits, such as TTL circuits, manufacturers will quote the fan-out and fan-in for a given electrical module. The fan-out indicates how many downstream logic gates can be connected to a given output. Exceeding these limits will potentially cause signal distortion in analog circuits and circuit failure in digital circuits.

We envision the development of similar criteria for connecting two biological modules together in synthetic biology, and here introduce the notion of fan-out for a genetic circuit. We define the fan-out of a genetic circuit as the maximum number of downstream promoters that can be driven from an upstream circuit signal without significant time-delay or signal attenuation. We will show that the fan-out can be estimated by using the autocorrelation [15–20] of gene expression noise [21–24]. During the estimation procedure the system’s retroactivity can also be measured. This fan-out/retroactivity estimation can be applied under quite general module interface conditions. Although our analysis is focused on genetic networks, the principles apply equally to signal transduction networks.

Results and Discussion

Module interface process

When two synthetic gene circuits are connected, transcription factors are used to connect them. The reaction processes involving the transcription factors such as transcription, translation, degradation, and downstream-module promoter regulation, will be called *module interface processes* (MIPs). For example, consider the repressilator [25]. Let us choose the TetR repressor, one of the genes comprising the oscillator, as an output of the oscillator module (Fig. 1). When a downstream module has *tetR*-operons, the MIP includes *tetR*-transcription, translation, and TetR binding/unbinding to its specific operons located in the

downstream module.

Retroactivity and mapping between a module interface process and an RC-circuit

We will investigate a MIP by mapping it to a simple electric circuit composed of a resistor and a capacitor connected in series (RC circuit). This mapping becomes significantly helpful for understanding retroactivity [14] and quantifying fan-out.

Isolated case

When an upstream output does not regulate any downstream promoter, we can model the corresponding MIP as a simple TF translation-degradation process (see Fig. 2A and B). The concentration of the TF, denoted by X , changes in time by following the equation

$$\frac{dX}{dt} = \alpha(t) - \gamma X, \quad (1)$$

with $\alpha(t)$ the translation rate and γ the degradation rate constant. We will show how this process can be related to an RC circuit, where a resistor and capacitor are connected in series and driven by an input voltage source V_{in} (Fig. 2C). The total voltage drop across both the resistor and capacitor is equal to the driven voltage: $V_{in} = RI + V_{out}$, where I denotes the current flowing through the resistor, and V_{out} the voltage drop across the capacitor. The current is equal to the rate of charge accumulation (Q) in the capacitor: $I = dQ/dt$, where the small increment dQ causes the change in V_{out} in proportion to dQ : $dQ = CdV_{out}$, with C a proportionality constant called capacitance. Thus, the current I can be expressed as CdV_{out}/dt . By substituting this into $V_{in} = RI + V_{out}$ and dividing the resultant equation by RC , we obtain

$$\frac{dV_{out}}{dt} = \frac{V_{in}}{RC} - \frac{V_{out}}{RC}, \quad (2)$$

where RC is known as the response time τ_0 of the RC-circuit [26]. By comparing Eqs. (1) and (2), we obtain the following correspondence: $X = V_{out}$, $\alpha = V_{in}/RC$, and $\gamma = 1/RC$, and the response time is expressed as

$$\tau_0 = RC = \frac{1}{\gamma}. \quad (3)$$

Thus, the TF-translation-degradation process (Fig. 2B) can be directly mapped to the RC-circuit (Fig. 2C).

Connected case

Now we consider the case where two modules are connected (see Fig. 3A). We will review retroactivity studied by Del Vecchio et al. [14]. The retroactivity was defined as the slow-down in interfacial dynamics in response to interactions with downstream components. The retroactivity described a number between zero and one with one being the least desirable, i.e. the interfacial dynamics are affected most. In their analysis, they assumed that the binding-unbinding process of the TF is fast enough that the process can be approximated to be in the quasi-steady state ($k_{on}X + k_{off} \gg \gamma$; cf. [27–29]). They also assumed that the lifetime of the bound TF is much longer than that of the unbound TFs.

Specifically, they showed that the free TF concentration X changes in time by the following equation [14]

$$\frac{dX}{dt} = (1 - \mathcal{R}(X))(\alpha - \gamma X), \quad (4)$$

where $\mathcal{R}(X)$ is the *retroactivity*, given by $\left[1 + \left(1 + \frac{X}{K_d}\right)^2 \frac{K_d}{P_T}\right]^{-1}$, with K_d the dissociation constant for the TF with respect to the promoter, and P_T the total number of the promoters. They showed that \mathcal{R} is always less than 1 and non-negative. The extra factor $1 - \mathcal{R}$ appears when compared with the isolated case, resulting in the slow-down of the dynamics. More precisely, the slow-down is due to the decrease in the factor placed in front of X in Eq. (4): $\gamma(1 - \mathcal{R})$, which is related to the apparent response time:

$$\tau_a \equiv \frac{1}{(1 - \mathcal{R})\gamma}. \quad (5)$$

We will consider the MIP shown in Figs. 3A and B under the same assumptions as given by Del Vecchio et al [14]. To understand the retroactivity by using an RC-circuit analogy, consider a circuit as shown in Fig. 3C. The total capacitance becomes the sum of the two capacitances: $C_T = C + C'$. Thus, the response time becomes RC_T : $\tau = RC_T$. The change in the output voltage is governed by the same equation as in the isolated case except the capacitance C is replaced to C_T :

$$\frac{dV_{out}}{dt} = \frac{V_{in}}{RC_T} - \frac{V_{out}}{RC_T} = \left[1 - \frac{C'}{C + C'}\right] \left[\frac{V_{in}}{RC} - \frac{V_{out}}{RC}\right]. \quad (6)$$

By comparing Eqs. (4) and (6), we find that the retroactivity is given by the relative ratio of the new capacitance:

$$\mathcal{R} = \frac{C'}{C + C'}, \quad (7)$$

and that the response time τ corresponds to τ_a (Eq. (5)):

$$\tau = RC_T = \frac{1}{(1 - \mathcal{R})\gamma}. \quad (8)$$

We have shown that connecting downstream promoters in the MIP is equivalent to connecting extra capacitors in parallel with an existing one in the RC-circuit. Due to these extra capacitors, the circuit takes a longer time to fully charge all the capacitors, resulting in the slow-down in the circuit response time. Biologically, the bound promoters act as a reservoir of potentially free TFs: Whenever there is a change in the number of the free TFs, the reservoir quickly buffers the change in the number of free TFs [30]. Such buffering causes transient dynamics at the interface to slow down.

Response time vs. number of promoters

We now investigate how the response time τ is related to the total number of promoters P_T . The response time is shown to increase with P_T (see the Methods section) as

$$\tau_{P_T} = R(C + P_T C_1), \quad (9)$$

where C_1 is a proportionality constant satisfying $C/C_1 = K_d(1 + X/K_d)^2$. The above equation (9) can be viewed as each individual promoter contributing an extra capacitance C_1 to the total capacitance (Fig. 3C): $C_T = C + P_T C_1$. The capacitance C_1 of each extra capacitor is related to a unit load onto the upstream output dynamics from a single downstream promoter. This is an interesting result and becomes useful for proposing an experimental method for estimating the fan-out.

The linear relationship between the extra capacitance and P_T (see Fig. 3C box) does not come from any linearization approximation, but from the fact that each downstream promoter affects the upstream as an independent effector (reservoir or sequestrator), although the sequestration itself is represented by a nonlinear reaction.

Gene circuit fan-out

We will define a gene circuit fan-out by the maximum number of promoters in a downstream module that the output (transcription factor) of an upstream module can regulate without

altering the output dynamics significantly. To exemplify how much the upstream module can be affected, we consider a repressilator [25] as a module and its Tet repressors as a module output (Fig. 1A). When the output regulates *tetR* promoters located in a downstream module, the oscillation amplitude of the *tetR* expression level can be significantly changed, e.g., 40% decrease when the number of the promoter (P_T) is changed from 0 to 100 (Fig. 1B and C). Our interest is here to quantify the maximum number of the promoters (fan-out) that the upstream module can tolerate.

Let us quantify the fan-out by considering again the simple MIP shown in Fig. 3A. We consider a frequency response between the input and output voltage, V_{in} and V_{out} , respectively (Fig. 4A). In the RC circuit, the capacitor acts as a low pass filter: The gain of the signal (the ratio of the oscillation amplitude of V_{out} to that of V_{in}) is at the maximum level for low frequencies and drops significantly when the circuit no longer responds as fast as the input signal changes (Fig. 4B). The frequency when this happens is called *cut-off frequency* (ω_c) (Fig. 4B) and corresponds to the inverse of the response time: $1/RC_T$ [31].

If the upstream module functions as a synthetic oscillator, there will be a practical upper limit (ω_{max}) in the oscillator's frequency (e.g., for the repressilator, ω_{max} can be the inverse of the repressor lifetime = $\log(2)/10 \text{ min}^{-1} \sim 4 \text{ hour}^{-1}$ [25]). If ω_{max} is smaller than the cut-off frequency ω_c , the oscillator output will operate in a predictable manner and the output signal will be passed downstream without any significant signal loss. As the number of the downstream promoters increases, the total capacitance increases as shown in Eq. (9) and the cut-off frequency ($\omega_c = 1/RC_T$) decreases. For the cut-off frequency to be larger than the maximum operational frequency ω_{max} , the total number of the promoter must be smaller than a certain value, which will be called the *fan-out*. The fan-out denoted by $F_{\omega_{max}}$ is obtained where ω_c equals ω_{max} , i.e., $\omega_c = [R(C + P_T C_1)]^{-1} = \omega_{max}$:

$$F_{\omega_{max}} = \frac{C}{C_1} \left[\frac{1/\tau_0}{\omega_{max}} - 1 \right]. \quad (10)$$

In the fan-out equation (10), there are two unknown parameters: C/C_1 , and τ_0 . These can be experimentally estimated by performing two independent experiments with and without any downstream module. In each experiment we measure the corresponding response time: τ_0 and τ_{P_T} (by using gene expression noise as will be presented later in the Results section). Thus, one of the unknowns τ_0 can be estimated. How can we estimate the other unknown C/C_1 from τ_{P_T} ? If we know a priori the copy number of the promoters P_T , we can obtain

the value of C/C_1 from Eq. (9). If the promoters are placed on plasmids, the copy number of the plasmids can be estimated depending on what type of origin of replication is used, and thus the copy number of the promoters P_T can be known. By calculating τ_0/RC_1 , we can estimate the other unknown, C/C_1 .

Gene circuit fan-out in more general interfaces

Up to now we have considered a simple MIP without feedback and where the degradation rate is assumed to be first-order. Here we will consider the more general case and show that we can use the same or similar fan-out function as Eq. (10).

Oligomer under directed degradation and self-regulation

Consider that a TF, composed of n monomers, is tagged for degradation and that its transcription is self-regulated as shown in Fig. 5A. We can obtain the fan-out expressed by the same equation (10), where τ_0 is the time constant in the isolated case, given by the difference between the elasticities [32]: $1/\tau_0 = \epsilon_2 - \epsilon_1$, where $\epsilon_1 \equiv \partial v_1(x, \alpha)/\partial x$ and $\epsilon_2 \equiv \partial v_2(x)/\partial x$ (refer to the Methods section). This means that the fan-out can be estimated exactly in the same way as in the monomer case as shown in Fig. 3A. All the above results apply for the case that the *intermediate* reaction steps of the oligomerization and directed degradation are taken into account (refer to the SI).

Multiple promoters having different affinities

Consider the case that two different types of TF-specific promoter plasmids, having different affinities for the TF and different strength of the origin of replication. It is shown that the MIP can be mapped to an RC-circuit having two different capacitances connected in parallel to C as shown in Fig. 5B (see the Methods section). The fan-out of each promoter is shown to satisfy the following functional relationship between F_1 and F_2 (refer to the Methods section):

$$1/\omega_{max} = \tau_0(1 + F_1 \frac{C_1}{C} + F_2 \frac{C_2}{C}), \quad (11)$$

where F_i is the fan-out for promoter plasmids of the i -th kind, and C_i denotes the corresponding capacitance per plasmid. If there are N different kinds of promoter plasmids, we need to sum up all the capacitances in the above equation. We note that the fan-out is not a single number but is given by a functional relationship between F_i 's: We need to balance the number of plasmids of different kinds depending on its unit load on the retroactivity, i.e., C_i/C .

To obtain the fan-out function, we need to find three unknown parameters: τ_0 , C_1/C , and C_2/C . τ_0 can be estimated in the isolated case. C_i/C can be estimated in the case that only the i -th kind of promoter plasmids exists (under the assumption that the strength of each origin of replication is already known). These three independent experiments will suffice for estimating all the unknown parameters and proposing the fan-out function Eq. (11).

Multiple operators

Consider the case that the promoter region includes multiple operators specific to an output TF (e.g., O_1 , O_2 , and O_3) having different affinities (Fig.5C). Regardless the number of the operators, the same fan-out function as Eq. (10) is obtained (refer to the SI).

Two output signals

When two output TFs (X and Z) regulate a downstream promoter independently, i.e., if there is no overlap between the operator regions and somehow X does not interfere with the operator region of Z and vice versa, the fan-out corresponding to each output TF can be obtained.

We have shown that the fan-out function like Eqs. (10) and (11) can be obtained for each of individual cases given above. Furthermore, for all the combinations of these individual cases the fan-out functions apply.

Design scheme for fan-out enhancement

How can we increase the fan-out? Based on the fan-out equations (10), there are two ways: increasing C/C_1 or $1/\tau_0$. The way to increase the latter is to apply a negative feedback on the

translation of X (making ϵ_1 negative for the case shown in Fig. 5A, where $1/\tau_0 = \epsilon_2 - \epsilon_1$) and a positive feed-forward on the degradation rate (increasing ϵ_2). Since the enhanced degradation and negative feedback decrease the concentration level of X , to prevent this, it is desirable to amplify the translation rate (which makes ϵ_1 more negative). This is exactly the same mechanism proposed by Del Vecchio et al. [14] to reduce retroactivity; when the retroactivity is small, the upstream output dynamics does not slow down significantly by connecting the output to the downstream module, meaning that the load from downstream to the upstream is small enough that many replicates of the load can be applied to the upstream without slowing down the output dynamics significantly.

One of the mechanisms, inhibitory auto-regulation, is frequently found in *Escherichia coli* transcription factors regulating a set of operons, e.g., for amino-acid biosynthesis where a single TF may control multiple targets, likewise for flagella formation [33]. Such motifs are called sing-input-module motifs [33].

The concept of fan-out is not limited to gene regulatory circuits. In principle, as long as the same class of interface processes are found regardless of the type of biological systems, the fan-out and retroactivity concepts can be applied [14, 34]. For example, in the eukaryotic MAPK pathway, doubly phosphorylated MAPK can activate a number of downstream proteins and transcription factors in the nucleus. This MAPK regulation can be described by the module interface process similar to the one shown in Fig. 5B (in this case, many promoter plasmids instead of the two). In the MAPK pathway, there is a negative feedback from MAPK to the phosphorylation of MAPKKK [11, 12]. The negative feedback increases the fan-out of the MAPK module thereby permitting MAPK to effectively regulate multiple targets and multiple homologous binding sites.

How to measure the time constant τ

It is known that transcription factors show significant stochastic fluctuations [17–20, 35–38] (for review articles, [21–24]). Their correlation times have been measured by obtaining autocorrelations by *in vivo* time-lapse microscopy [17–20]. Recent numerical studies show that the correlation time is approximately equal to the response time of the deterministic case [39] and that it changes as a result of connecting two genetic systems [39, 40]. Therefore, by using the change in the correlation time, we can estimate the fan-out by using Eq. (10)

as well as the retroactivity by using $\mathcal{R} = \frac{\tau_{P_T} - \tau_0}{\tau_{P_T}}$ (obtained from Eq. (7) by using Eqs. (3) and (8)).

Example: Fan-out/retroactivity estimation

Let us consider the simple MIP shown in Fig. 3A as a model for TFs in *E. coli*. We consider that the average copy number of plasmids containing the specific promoters ranges from 1 to 100. If we set the volume of *E. coli* roughly equal to $1\mu\text{m}^3$, a copy number of one corresponds to 1 nM. As a result we will henceforth interchange the unit of nM with that of copy number. A simulation using the standard Gillespie method [41] was performed and the observed autocorrelation was fitted to an exponential function: $G(\Delta t) = A \exp(-\Delta t/\tau)$ with τ a correlation time (we conducted a linear fit in the log-scale in the y -axis and the normal scale in the x -axis) and $1/\tau$ obtained from the fitted slope.

For experimentally reasonable parameter values, i.e., $\alpha = 20 \text{ nM hour}^{-1}$, $\gamma = 2 \text{ hour}^{-1}$, $k_{on} = 10 \text{ nM}^{-1}\text{hour}^{-1}$, and $k_{off} = 10 \text{ hour}^{-1}$, we performed the stochastic simulations with and without any downstream-module promoter ($P_T = 100$ and 0). The concentration levels of the total TF was recorded 100 times over 2 hours, the autocorrelation of this signal fitted to an exponential function, and the response time measured [39]. We obtained the error bar of the time constant from 10 independent replicates of the autocorrelation.

When the translation rate was set to 20 nM hour^{-1} , we obtained $\tau_0 = 0.52 \pm 0.06 \text{ hour}$ and $\tau_{100} = 0.9 \pm 0.1 \text{ hour}$. We obtained $C/C_1 = 140 \pm 20$, by using

$$\frac{C}{C_1} = P_T \frac{RC}{RC_T - RC} = P_T \frac{\tau_0}{\tau_{P_T} - \tau_0} \Big|_{P_T=100},$$

where we used $C_T - C = P_T C_1$. From Eq. (10), we obtained the fan-out function for this MIP:

$$F_{\omega_{max}} = 140[\pm 20] \left(\frac{1/0.9[\pm 0.1]}{\omega_{max}} - 1 \right).$$

If the upstream module is a synthetic oscillator with a maximum operating frequency $\omega_{max} = 1 \text{ hour}^{-1}$, the fan-out becomes $F = 130 \pm 20$. This means that we can use promoter plasmids with low, medium, and high copy numbers without affecting the TF dynamics, if a single TF-specific operator site resides on a plasmid. The retroactivity can also be estimated from the measured values of τ_0 and τ_{100} : $\mathcal{R} = 0.4 \pm 0.1$.

If we reduce the translation rate by half (now, $\alpha = 10 \text{ nM hour}^{-1}$) the free TF concentration decreases by half. As the concentration decreases, the retroactivity increases [14, 39] and the fan-out decreases. We estimated $\tau_0 = 0.52 \pm 0.07 \text{ hour}$ and $\tau_{100} = 1.75 \pm 0.04 \text{ hour}$. For the same $\omega_{max} = 1 \text{ hour}^{-1}$ we obtained the fan-out: $F = 40 \pm 1$. This would mean that we could safely use only low copy number plasmids. The retroactivity is estimated to be 0.70 ± 0.05 .

Conclusions

In this paper we have introduced the concept and quantitative measure of fan-out for genetic circuits which is a measure of the maximum number of promoter sites that the output TFs of the upstream module can regulate without significant slow-down in the kinetics of the output. In addition we have also proposed an efficient method to estimate the fan-out experimentally. We have shown that the fan-out can be enhanced by self-inhibitory regulation on the output. In the estimation process of the fanout, the retroactivity can also be estimated. This study provides a way for quantifying the level of modularity in gene regulatory circuits and helps characterize and design module interfaces and therefore the modular construction of gene circuits.

Methods

We obtain the time-constant τ_{P_T} and derive the fan-out functions for various cases.

Monomer TF

Consider the simple MIP shown in Fig. 3. Under the quasi-equilibrium in the binding-unbinding process, we obtain the concentration of the bound TF as $P_b = P_T X / (X + K_d)$. We will simplify this equation to, by introducing $f(X) \equiv X / (X + K_d)$,

$$P_b = P_T f(X). \quad (12)$$

The time evolution of the total transcription factor ($Y = X + P_b$) is governed by the following equation [39]:

$$\frac{dY}{dt} = \alpha - \gamma X.$$

We will obtain the response time constant of Y rather than X , because Y is a pure slow variable showing the dynamics of our interest [14, 28, 39]. We denote the response time constant of Y by τ_{P_T} , and is obtained by taking the derivative on the right hand side of the above equation with respect to Y :

$$\tau_{P_T} = - \left[\frac{d(\alpha - \gamma X)}{dY} \right]^{-1} = \tau_0 \frac{dY}{dX}, \quad (13)$$

with $\tau_0 \equiv \gamma^{-1}$. By using $Y = X + P_b$, the above equation becomes $\tau_{P_T} = \tau_0 \left[1 + \frac{dP_b}{dX} \right]$. By using Eq. (12), we obtain the time constant: $\tau_{P_T} = \tau_0(1 + f'(X)P_T)$. By comparing this with Eq. (9) we obtain $C/C_1 = K_d(1 + X/K_d)^2$.

Oligomer TF under directed degradation and self-regulation

We consider that the transcription factors are composed of n monomers described in Fig. 5A. We assume that the binding-unbinding process is in equilibrium, and we obtain P_b as

$$P_b = \frac{P_T X^n}{X^n + K_d} \equiv P_T f(X).$$

The time evolution of $Y (= X + nP_b)$ is governed by

$$\frac{dY}{dt} = v_1(X) - v_2(X).$$

The response time constant of Y is obtained as

$$\tau_{P_T} = - \left[\frac{d[v_1(X) - v_2(X)]}{dY} \right]^{-1} = \tau_0 \frac{dY}{dX},$$

where $\tau_0 \equiv 1/(\epsilon_2 - \epsilon_1)$ with $\epsilon_1 \equiv \partial v_1/\partial X$ and $\epsilon_2 \equiv dv_2(X)/dX$. By using $Y = X + nP_b$, we obtain

$$\tau_{P_T} = \tau_0 \left[1 + P_T n \frac{df(X)}{dX} \right],$$

where $n \frac{df(X)}{dX}$ is defined to be C_1/C by comparing the above equation with Eq. (9).

Multiple promoters having different affinities

We consider the case that two different types of TF-specific promoter plasmids, having different affinities for the TF and different strength of the origin of replication. The TF is

assumed to be a monomer. The concentration of the TF bound on the promoter of each type (i) is given as $P_{bi} = \frac{P_{Ti}X}{X+K_{di}} \equiv P_{Ti}f_i(X)$ for $i = 1, 2$. The response time constant $\tau_{P_{T1}, P_{T2}}$ is given by Eq. (13). By using $Y = X + P_{b1} + P_{b2}$, we obtain $\tau_{P_{T1}, P_{T2}} = \tau_0 \left[1 + \frac{dP_{b1}}{dX} + \frac{dP_{b2}}{dX}\right]$, and rewrite this as $\tau_{P_{T1}, P_{T2}} = \tau_0 [1 + f'_1(X)P_{T1} + f'_2(X)P_{T2}]$ by using $P_{bi} = P_{Ti}f_i(X)$. Finally by equating $\tau_{P_{T1}, P_{T2}}$ to $1/\omega_{max}$, we obtain Eq. (11). If there were n -different types of promoter plasmids, the above equation is changed by replacing the last two terms to the sum over all the n -types.

In the RC-circuit representation, $\tau_{P_{T1}, P_{T2}}$ is given by RC_T and the total capacitance C_T is obtained as $C_T = C + C_1P_{T1} + C_2P_{T2}$ with $C_i = \tau_0 f'_i(X)/R$. This indicates that this MIP can be mapped to an RC-circuit having two different capacitances connected in parallel to C as shown in Fig. 5B.

Competing interests

The authors declare that they have no competing interests.

Authors contributions

KHK primarily developed and carried out the proposed work. HS participated its design and provided critical feedback and suggestions. All authors read and approved the final manuscript.

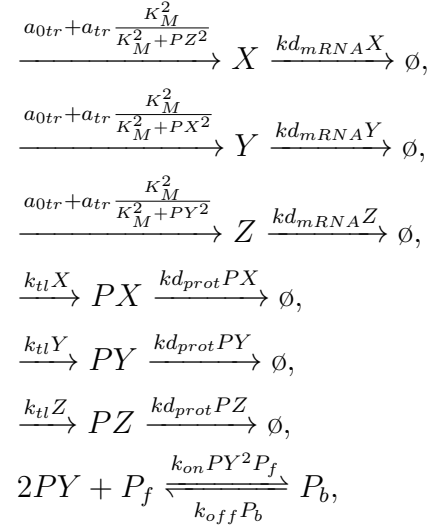
Acknowledgments

This work was supported by a National Science Foundation (NSF) Grant in Theoretical Biology 0827592. Preliminary studies were supported by funds from NSF FIBR 0527023. The authors acknowledge useful discussions with Hong Qian and Suk-jin Yoon.

Supplementary Information

I. REPRESSILATOR BIOMODEL

We obtained a model for the repressilator from the BioModels Database (model id: BIOMD0000000012) [42]. This model is composed of transcription and translation processes for respective *lacI*, *tetR*, and *cI*. Inhibitory regulations among them are described by Hill functions. One of the repressors, TetR, is chosen as an output of the repressilator module. The TetR repressors are allowed to regulate a downstream module and its regulation is described by the binding-unbinding reactions between the TetR and its specific promoter located in the downstream module. The copy numbers of mRNAs of respective *lacI*, *tetR*, and *cI* are denoted by X , Y , and Z , and the corresponding repressor molecules by PX , PY and PZ . The model process (per cell) is described as,



where the total number P_T of the *tetR* promoter in the downstream module is given by the sum of the numbers of the free and bound promoters: $P_f + P_b$. We have assumed that the transcription and translation processes for each repressor gene are identical. The parameter values used for simulations are listed in Table I. We have modified the parameters to increase the retroactivity by reducing the expression levels of the repressor molecules ($a_{tr} : 29.97 \rightarrow 2.97$, $K_M : 40 \rightarrow 10$, $eff : 20 \rightarrow 10$).

a_{0tr}	0.03 min^{-1}	Basal transcription rate
a_{tr}	$3 - 0.03 = 2.97 \text{ min}^{-1}$	Maximum transcription rate is set to 3 min^{-1} .
K_M	10	Number of repressor molecules corresponding to the half maximal transcription
kd_{mRNA}	$\frac{\log(2)}{\tau_{mRNA}} \text{ min}^{-1}$	Degradation rate constant of mRNA
τ_{mRNA}	2 min	Half life time of mRNA
k_{tl}	$eff \frac{\log(2)}{\tau_{mRNA}} \text{ min}^{-1}$	Translation rate per mRNA
eff	10	Translation efficiency: Number of repressor molecules translated per mRNA during mRNA life time
kd_{prot}	$\frac{\log(2)}{\tau_{prot}} \text{ min}^{-1}$	Degradation rate constant of repressor molecules
τ_{prot}	10 min	Repressor molecule half life time
k_{on}	0.166 min^{-1}	Promoter-repressor binding constant [38]
k_{off}	1.66 min^{-1}	Promoter-repressor unbinding constant for a given dissociation constant $K_d = k_{off}/k_{on} = 10$
P_T	0 or 100	Number of <i>tetR</i> promoters in a downstream module

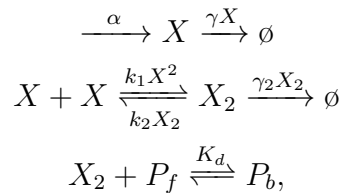
TABLE I: Parameters of the repressilator BioModel

II. LINEAR RELATIONSHIP BETWEEN C' AND P_T

In this section, we consider the case that the *intermediate* reaction steps of oligomerization and enzyme-mediated degradation are taken into account.

A. Oligomer TF

We consider a dimer TF (the results obtained below can be generalized to any other oligomer types). The corresponding model can be expressed as:



where the reactions from the top represent the monomer translation and degradation, dimerization, dimer degradation, and promoter-binding-unbinding reactions. K_d denotes the dissociation constant. The time evolution of the total transcription factor (monomer units) ($Y = X + 2X_2 + 2P_b$) is governed by

$$\frac{dY}{dt} = \alpha - \gamma X - 2\gamma_2 X_2.$$

The response time constant of Y becomes

$$\tau_{P_T} = - \left[\frac{d(\alpha - \gamma X - 2\gamma_2 X_2)}{dY} \right]^{-1} = \left[\gamma \frac{dX}{dY} + 2\gamma_2 \frac{dX_2}{dY} \right]^{-1}. \quad (14)$$

Under the assumption of the equilibrium of X_2 and P_b , we obtain

$$X_2 = \frac{k_1}{k_2 + \gamma_2} X^2, \quad \text{and} \quad P_b = \frac{P_T X_2}{K_d + X_2} \equiv P_T f(X). \quad (15)$$

By substituting the first equation in the above to Eq. (14), we obtain

$$\tau_{P_T} = \left[\gamma + \frac{4\gamma_2 k_1 X}{k_2 + \gamma_2} \right]^{-1} \frac{dY}{dX}$$

By using $Y = X + 2X_2 + 2P_b$ and Eq. (15), we obtain

$$\tau_{P_T} = \tau_0 \left[1 + \frac{2f'(X)}{1 + \frac{4k_1 X}{k_2 + \gamma_2}} P_T \right], \quad (16)$$

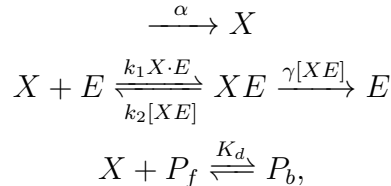
where τ_0 denotes the time constant in the case without any promoter:

$$\tau_0 = \frac{1 + \frac{4k_1 X}{k_2 + \gamma_2}}{\gamma + \frac{4\gamma_2 k_1 X}{k_2 + \gamma_2}}.$$

We note that the steady state concentration of X is independent of P_T . Equation (16) shows that the extra capacitance C' is proportional to P_T (by noting that $\tau_{P_T} = RC_T = R(C + C')$ and $\tau_0 = RC$).

B. Degradation-tagged TF

We consider a monomer TF under directed degradation by proteases. The corresponding model can be expressed as:



with the total number of the proteases $E_T (= E + [XE])$ fixed. The time evolution of the total TF ($Y = X + [XE] + P_b$) is governed by

$$\frac{dY}{dt} = \alpha - \gamma[XE].$$

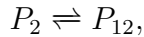
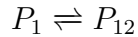
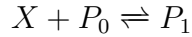
The response time constant of Y becomes

$$\tau_{P_T} = - \left[\frac{d(\alpha - \gamma[XE])}{dY} \right]^{-1} = \left[\gamma \frac{d[XE]}{dY} \right]^{-1}.$$

Under the assumption of the equilibrium of $[XE]$ and P_b , we can express $[XE]$ and P_b in terms of X as like Eq. (15). By following the same way as above, we can prove that the time constant increases by the amount proportional to P_T as like Eq. (16).

C. Multiple operators

Consider a dimer TF that can bind two operator sites with different affinities. The binding-unbinding process between the TF and the promoter can be modeled as



where P_0 , P_i , and P_{12} denote promoters that are free, occupied at the i -th operator site, and fully occupied, respectively. The equilibrium constant of each reaction from top to bottom is denoted by K_1 , K_2 , K_3 , and K_4 . By using that the total promoter concentration P_T equals $P_0 + P_1 + P_2 + P_{12}$, we obtain

$$P_b \equiv P_1 + P_2 + P_{12} = \frac{P_T X}{X + K_d} \equiv P_T f(X), \quad (17)$$

where

$$K_d \equiv [K_1 + K_2 + K_1/K_3]^{-1}.$$

We note that $K_1/K_3 = K_2/K_4$. The response time constant τ_{P_T} , given by

$$\tau_{P_T} = - \left[\frac{d(\alpha - \gamma X)}{dY} \right]^{-1} = \tau_0 \frac{dY}{dX},$$

is re-written as

$$\tau_{P_T} = \tau_0(1 + f'(X)P_T). \quad (18)$$

by using $Y = X + P_b$. If there were n -operators and the TF is an oligomer, the same derivation can be applied resulting in Eq. (18).

-
- [1] Lancaster DE: *TTL Cookbook*. Sams 1980.
 - [2] Alon U: **Network motifs: theory and experimental approaches**. *Nat. Rev. Genet.* 2007, **8**(6):450–461.
 - [3] Purnick PEM, Weiss R: **The second wave of synthetic biology: from modules to systems**. *Nat. Rev. Mol. Cell Biol.* 2009, **10**(6):410–422.
 - [4] Lucks JB, Qi L, Whitaker WR, Arkin AP: **Toward scalable parts families for predictable design of biological circuits**. *Curr. Opin. Microbiol.* 2008, **11**(6):567–573.
 - [5] Keasling JD: **Synthetic biology for synthetic chemistry**. *ACS Chem. Biol.* 2008, **3**:64–76.
 - [6] Voigt CA: **Genetic parts to program bacteria**. *Curr. Opin. Biotechnol.* 2006, **17**(5):548–557.
 - [7] Sprinzak D, Elowitz MB: **Reconstruction of genetic circuits**. *Nature* 2005, **438**(7067):443–448.
 - [8] Endy D: **Foundations for engineering biology**. *Nature* 2005, **438**(7067):449–453.
 - [9] Hasty J, McMillen D, Collins JJ: **Engineered gene circuits**. *Nature* 2002, **420**(6912):224–230.
 - [10] Stelling J, Sauer U, Szallasi Z, Doyle III FJ, Doyle J: **Robustness of cellular functions**. *Cell* 2004, **118**(6):675–685.
 - [11] Sauro HM, Kholodenko BN: **Quantitative analysis of signaling networks**. *Prog. Biophys. Mol. Biol.* 2004, **86**:5–43.
 - [12] Sauro HM, Ingalls B: **MAPK cascades as feedback amplifiers**. *arXiv:0710.5195[q-bio.MN]* 2007.
 - [13] Saez-Rodriguez J, Kremling A, Gilles ED: **Dissecting the puzzle of life: modularization of signal transduction networks**. *Comput. Chem. Eng.* 2005, **29**(3):619–629.
 - [14] Del Vecchio D, Ninfa AJ, Sontag ED: **Modular cell biology: retroactivity and insulation**. *Mol. Syst. Biol.* 2008, **4**:161.

- [15] Anishchenko VS, Astakhov V, Neiman A, Vadivasova T, Schimansky-Geier L: *Nonlinear dynamics of chaotic and stochastic systems*. Springer-Verlag 2002.
- [16] Simpson ML, Cox CD, Sayler GS: **Frequency domain analysis of noise in autoregulated gene circuits**. *Proc. Natl. Acad. Sci. U. S. A.* 2003, **100**(8):4551.
- [17] Rosenfeld N, Young JW, Alon U, Swain PS, Elowitz MB: **Gene regulation at the single-cell level**. *Science* 2005, **307**(5717):1962–1965.
- [18] Austin DW, Allen MS, McCollum JM, Dar RD, Wilgus JR, Sayler GS, Samatova NF, Cox CD, Simpson ML: **Gene network shaping of inherent noise spectra**. *Nature* 2006, **439**:608–611.
- [19] Weinberger LS, Dar RD, Simpson ML: **Transient-mediated fate determination in a transcriptional circuit of HIV**. *Nat. Genet.* 2008, **40**(4):466–470.
- [20] Dunlop MJ, Cox III RS, Levine JH, Murray RM, Elowitz MB: **Regulatory activity revealed by dynamic correlations in gene expression noise**. *Nat. Genet.* 2008, **40**(12):1493–1498.
- [21] Rao CV, Wolf DM, Arkin AP: **Control, exploitation and tolerance of intracellular noise**. *Nature* 2002, **420**(6912):231–237.
- [22] Raser JM, O’Shea EK: **Control of stochasticity in eukaryotic gene expression**. *Science* 2004, **304**(5678):1811–1814.
- [23] Kærn M, Elston TC, Blake WJ, Collins JJ: **Stochasticity in gene expression: from theories to phenotypes**. *Nat. Rev. Genet.* 2005, **6**(6):451–464.
- [24] Shahrezaei V, Ollivier JF, Swain PS: **Colored extrinsic fluctuations and stochastic gene expression**. *Mol. Syst. Biol.* 2008, **4**:196.
- [25] Elowitz MB, Leibler S: **A synthetic oscillatory network of transcriptional regulators**. *Nature* 2000, **403**(6767):335–338.
- [26] [The solution of Eq. (1) with α constant is given by $X(t) = (X(0) - \alpha/\gamma) e^{-\gamma t} + \alpha/\gamma$, with $X(0)$ the initial concentration. Thus, the exponential function decreases sufficiently at $t \simeq 1/\gamma$.].
- [27] Kepler TB, Elston TC: **Stochasticity in transcriptional regulation: origins, consequences, and mathematical representations**. *Biophys J* 2001, **81**(6):3116–3136.
- [28] Rao CV, Arkin AP: **Stochastic chemical kinetics and the quasi-steady-state assumption: Application to the Gillespie algorithm**. *J. Chem. Phys.* 2003, **118**:4999.
- [29] Simpson ML, Cox CD, Sayler GS: **Frequency domain chemical Langevin analysis of stochasticity in gene transcriptional regulation**. *J. Theor. Biol.* 2004, **229**(3):383–394.

- [30] Buchler NE, Cross FR: **Protein sequestration generates a flexible ultrasensitive response in a genetic network.** *Mol Syst Biol* 2009, **5**:272.
- [31] Nilsson J, Riedel S: *Electric circuits*. Pearson Prentice Hall 2008.
- [32] Fell DA: **Metabolic control analysis: a survey of its theoretical and experimental development.** *Biochem. J.* 1992, **286**:313–330.
- [33] Shen-Orr SS, Milo R, Mangan S, Alon U: **Network motifs in the transcriptional regulation network of Escherichia coli.** *Nature Genet.* 2002, **31**:64–68.
- [34] Sauro HM: **Modularity defined.** *Mol. Syst. Biol.* 2008, **4**:166.
- [35] Arkin A, Ross J, McAdams HH: **Stochastic kinetic analysis of developmental pathway bifurcation in phage lambda-infected Escherichia coli cells.** *Genetics* 1998, **149**(4):1633–1648.
- [36] Elowitz MB, Levine AJ, Siggia ED, Swain PS: **Stochastic gene expression in a single cell.** *Science* 2002, **297**(5584):1183–1186.
- [37] Ozbudak EM, Thattai M, Kurtser I, Grossman AD, van Oudenaarden A: **Regulation of noise in the expression of a single gene.** *Nat Genet* 2002, **31**:69–73.
- [38] Elf J, Li GW, Xie XS: **Probing transcription factor dynamics at the single-molecule level in a living cell.** *Science* 2007, **316**(5828):1191–1194.
- [39] Kim KH, Sauro HM: **Measuring the degree of modularity from gene expression noise in gene regulatory circuits.** *arXiv:0910.5522[q-bio.MN]* 2009.
- [40] Jayanthi S, Vecchio DD: **On the Compromise between Retroactivity Attenuation and Noise Amplification in Gene Regulatory Networks.** *Proc. IEEE Conf. Dec. Control* 2009, :4565–4571.
- [41] Gillespie DT: **Exact stochastic simulation of coupled chemical reactions.** *J. Phys. Chem.* 1977, **81**:2340–2361.
- [42] Le Novère N, Bornstein B, Broicher A, Courtot M, Donizelli M, Dharuri H, Li L, Sauro H, Schilstra M, Shapiro B, Snoep JL, Hucka M: **BioModels Database: a free, centralized database of curated, published, quantitative kinetic models of biochemical and cellular systems.** *Nucleic Acids Res.* 2006, **34**(Database Issue):D689–D691.

Figure 1 – Gene circuit modules and their interface process

(A) The repressilator (Module 1) [25] regulates multiple copies of a downstream module (Module 2). The multiple copies can be realized by placing the downstream module in a plasmid. TetR repressors (output of Module 1) regulate their specific downstream-module promoters (input of Module 2). A module interface process (MIP) defines the collection of the processes of *tetR*-transcription and translation and its specific downstream-module regulation. As the number of the downstream-module promoter (P_T) increases, the amplitude and period of the oscillation in the repressilator can be changed (B and C). A repressilator model was obtained from the BioModels Database BIOMD0000000012 [42]. We modified the model to lower the expression levels (by changing translation efficiency to 10 and K_M to 10 and the maximum transcription rate to 3 per min per cell) and to add promoter binding-unbinding reactions for TetR repressors (for the detailed model description, refer to the SI).

Figure 2 – Isolated module output

Translation-degradation processes for X (A) can be described by a simple reaction process (B) with α a translation rate and γX a degradation rate. These processes can be mapped to an RC-circuit with R resistance and C capacitance by $V_{out} = X$, $V_{in} = \alpha/\gamma$, and $RC = 1/\gamma$ (C).

Figure 3 – Module interface process

The output X of an upstream module regulates the downstream-module X -specific promoter (A). The translation-degradation processes for X and its promoter regulation can be modeled as the reaction process shown in B, where P_f , P_b , and P_T denote the numbers of free, bound, and total promoters, respectively. The reaction process is mapped to an RC-circuit with an increased capacitance by C' , which is shown to be proportional to P_T : $C' = P_T C_1$ with C_1 a proportionality constant. This means that each promoter acts as a capacitor with a unit load of capacitance, C_1 . The total capacitance C_T becomes the sum of the capacitance C in the isolated case and the extra capacitance C' .

Figure 4 – Frequency response of the module interface process shown in Fig. 3A

An oscillatory signal is applied at V_{in} with different frequencies (A). The signal gain is defined by the ratio of the oscillation amplitude of the output signal (V_{out}) to that of the input (V_{in}): $g(\omega) = \frac{\Delta V_{out}(\omega)}{\Delta V_{in}(\omega)}$, and can be well approximated by $g(\omega) = \sqrt{1 + \omega^2 / (RC_T)^2}^{-1}$ [31] with C_T the total capacitance. As the number of the promoters that the output (TF) signal drives (regulates) increases, the cut-off frequency ($\omega_c = 1/RC_T$) decreases (B). We assume that the output signal is desired to be operated within a certain frequency range between 0 and 1 hour⁻¹, i.e., the maximum operating frequency ω_{max} is 1 hour⁻¹. When the cut-off frequency matches the maximum operating frequency, the corresponding number of the promoters is defined as the fan-out (C). Parameters of the model: $K_d = 1$ nM [$k_{on} = 10(1/\text{nM}/\text{hour})$, $k_{off} = 10$ (1/hour)], $\gamma = 2(1/\text{hour})$, $\alpha = 20(\text{nM}/\text{hour})$.

Figure 5 – Module interface processes that the fan-out function Eqs. (10) and (11) can be applied to

(A) An oligomer TF degraded by proteases. (B) A TF can bind two different promoter plasmids having different binding affinities and different origins of replication. This can be mapped to an RC-circuit with two different capacitances connected in parallel. (C) An Oligomer TF can bind multiple operators. (D) Each different TF binds to its specific operator without affecting the binding affinity of the other.

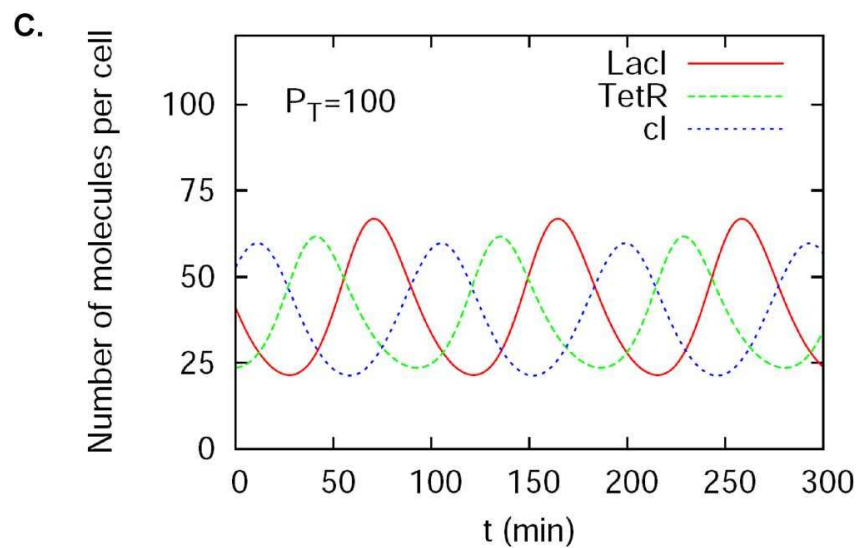
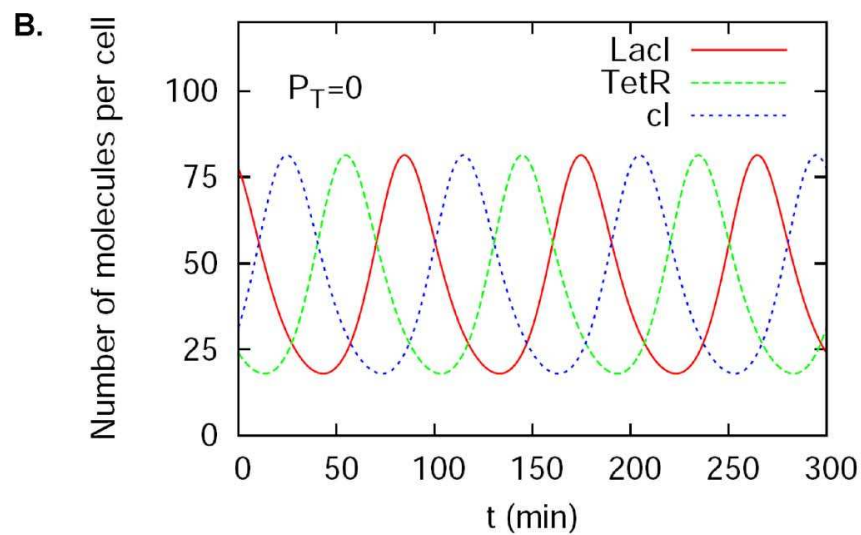
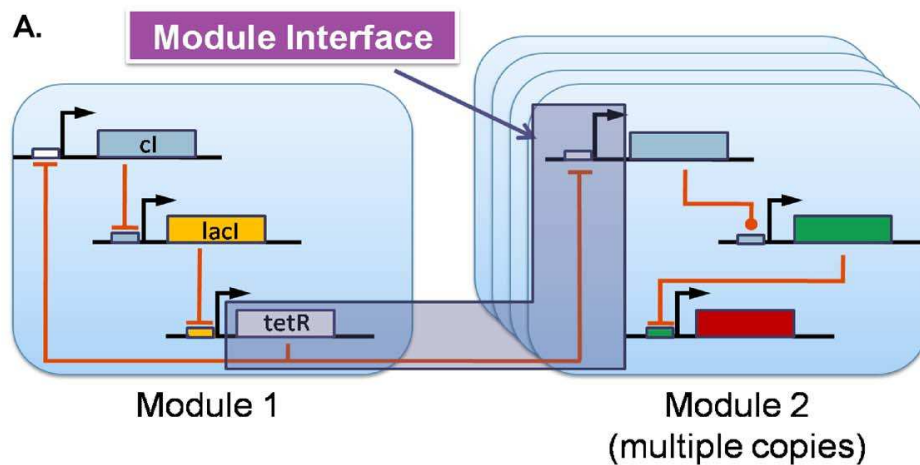


FIG. 1:

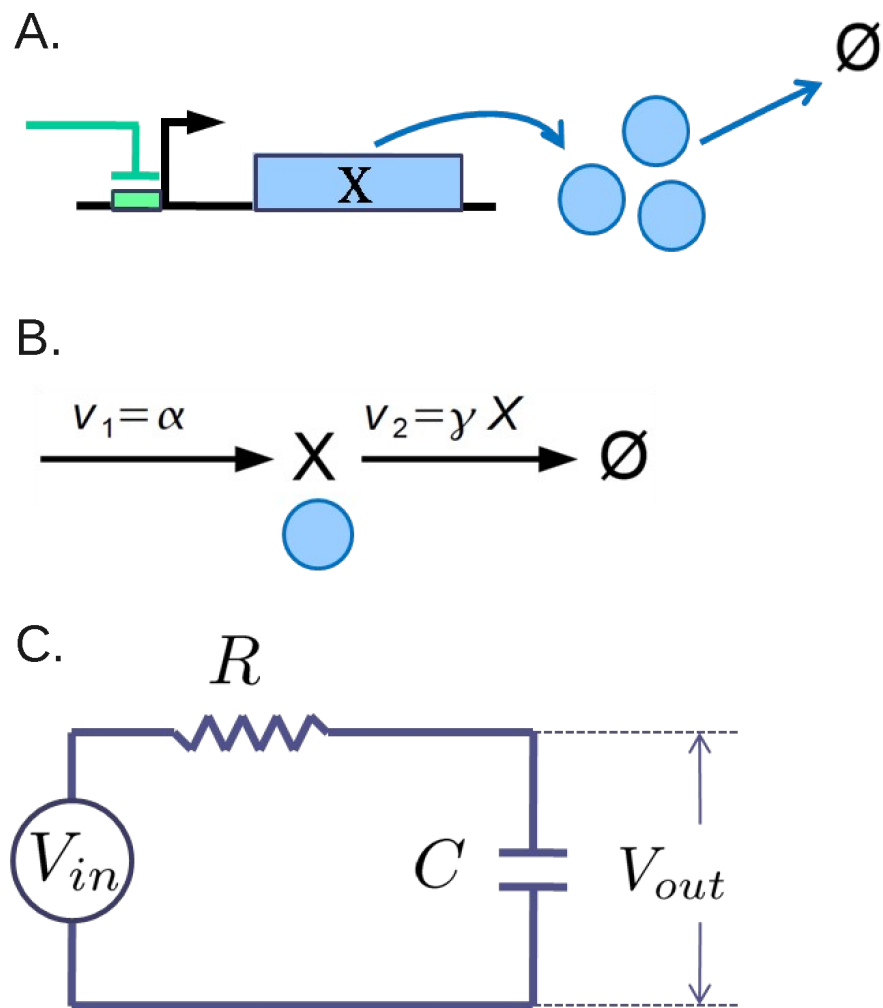


FIG. 2:

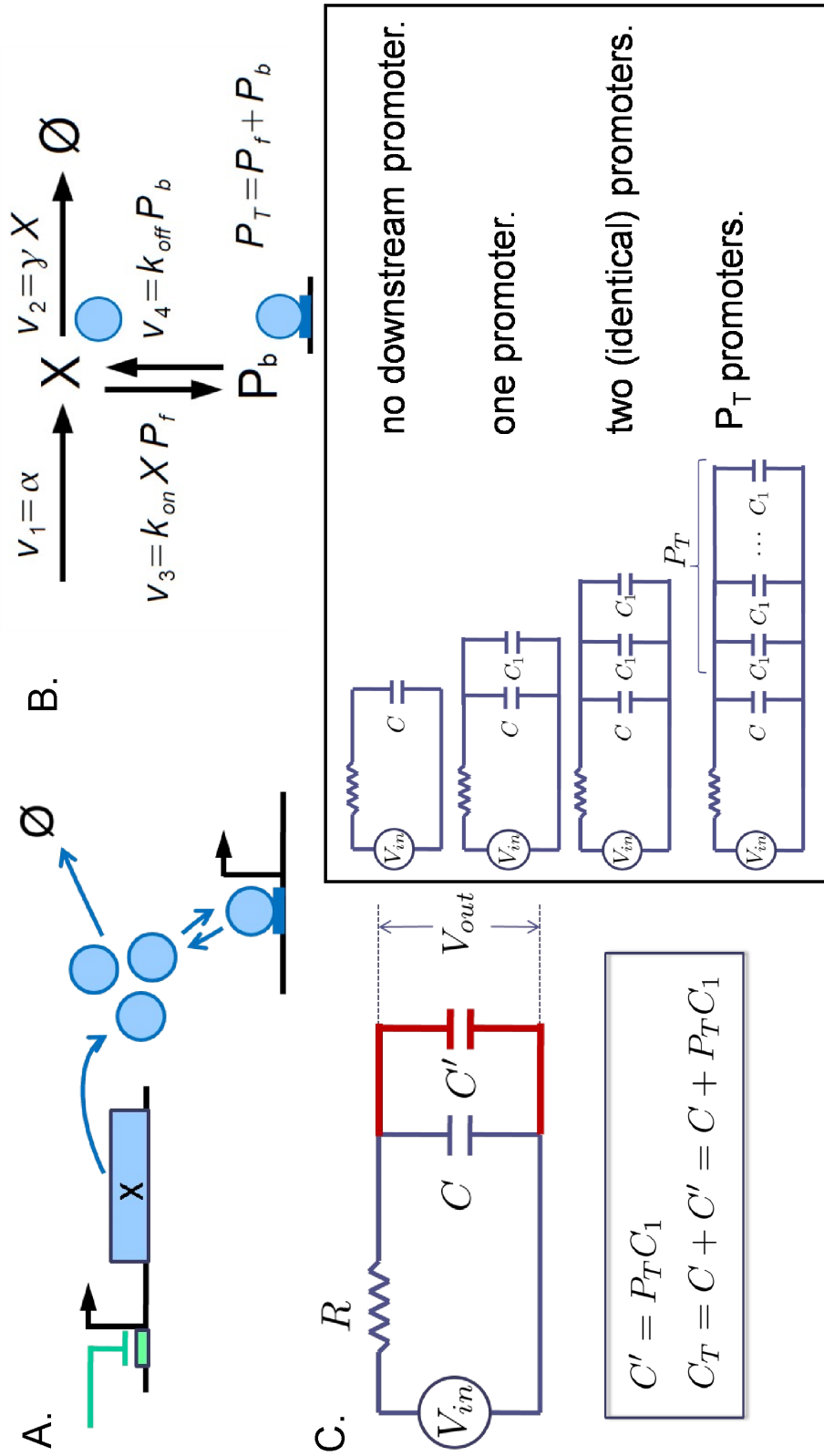


FIG. 3:

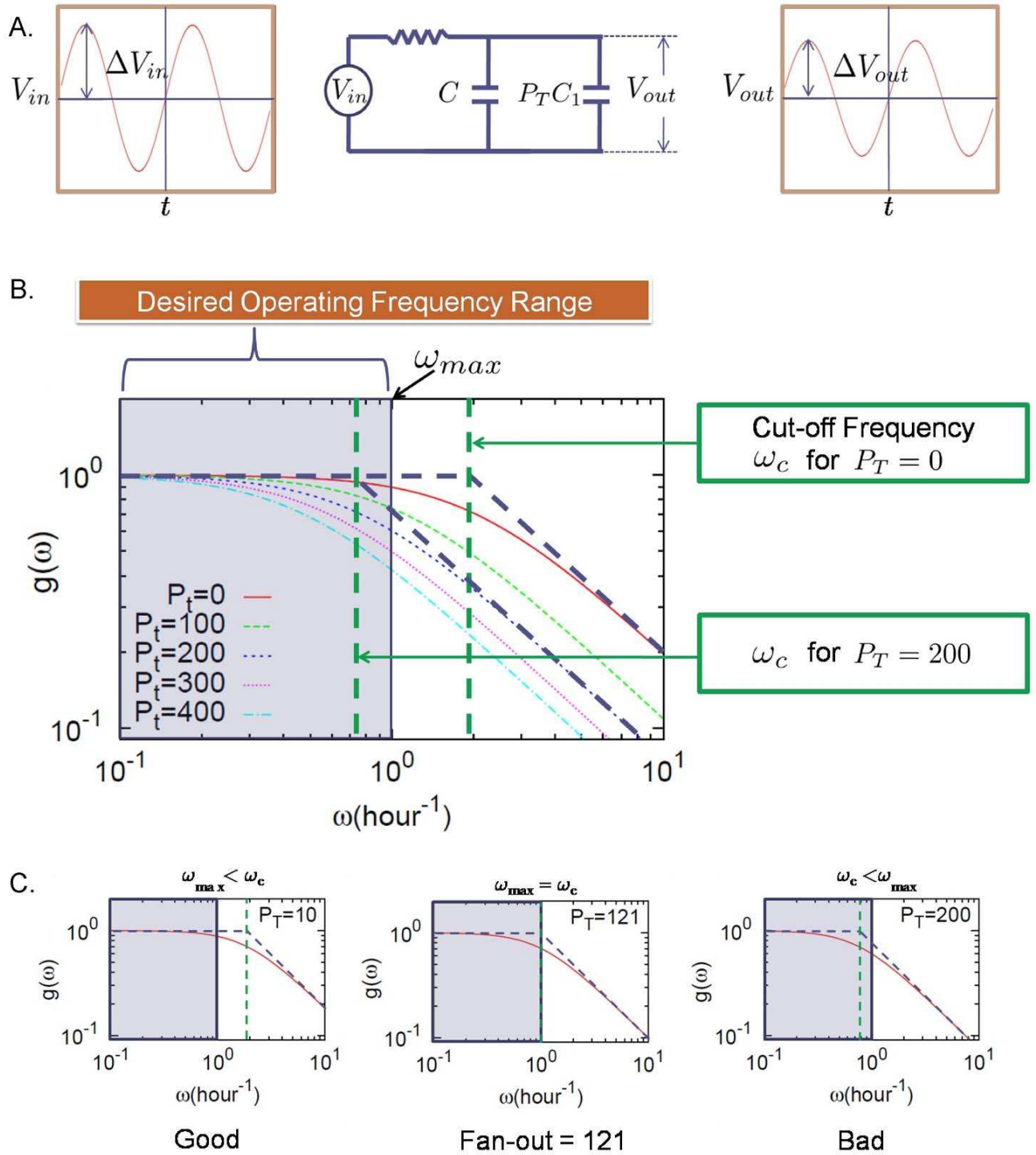


FIG. 4:

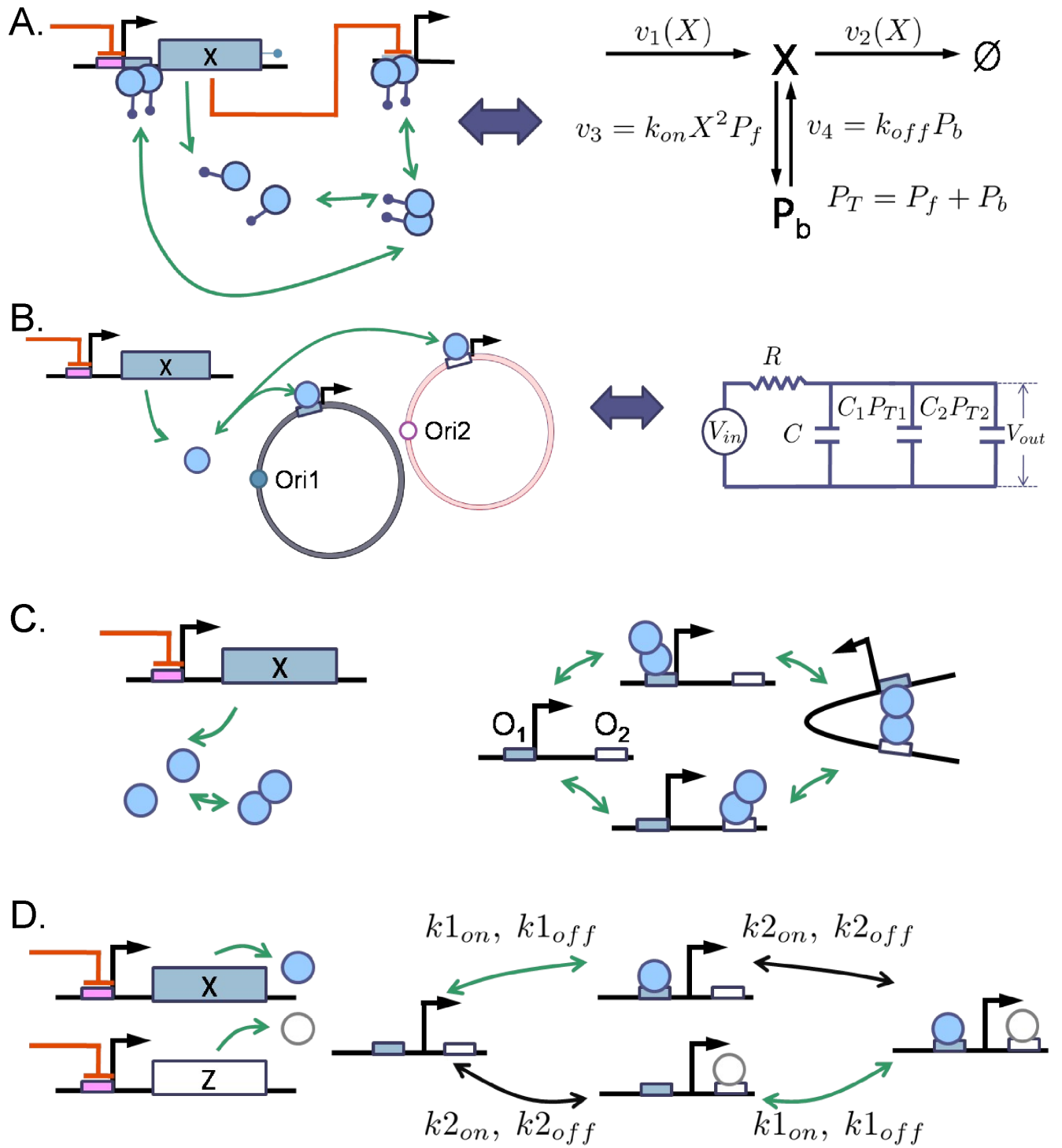


FIG. 5: